Available online at www.sciencedirect.com
ScienceDirect
Polar Science 2 (2008) 163–174
http://ees.elsevier.com/polar/

Rb–Sr, Sm–Nd, and Ar–Ar isotopic systematics of lherzolitic shergottite Yamato 000097

K. Misawa [a,b,*], J. Park [c], C.-Y. Shih [d], Y. Reese [e], D.D. Bogard [c], L.E. Nyquist [c]

[a] Antarctic Meteorite Research Center, National Institute of Polar Research, Tokyo 173-8515, Japan
[b] Department of Polar Science, Graduate University for Advanced Studies, Tokyo 173-8515, Japan
[c] ARES, Mail Code KR, NASA Johnson Space Center, Houston, TX 77058, USA
[d] ESCG/Jacobs Sverdrup, Houston, TX 77058, USA
[e] ESCG/Muñiz Engineering, Houston, TX 77058, USA

Received 17 September 2007; revised 10 July 2008; accepted 13 August 2008
Available online 11 September 2008

Abstract

Isotopic analysis of the Martian lherzolitic shergottite Yamato 000097 yields a Rb–Sr age of 147 ± 28 Ma with an initial $^{87}Sr/^{86}Sr$ ratio of 0.710490 ± 0.000072, a Sm–Nd age of 152 ± 13 Ma with an initial $\varepsilon^{143}Nd$-value of $+11.7 \pm 0.2$, and a ^{39}Ar–^{40}Ar age of ~260 Ma. The near concordance of these ages, in combination with the Rb–Sr and Sm–Nd initial isotopic signatures, suggests that Yamato 000097 crystallized from low Rb/Sr, light rare earth element depleted source materials ~150 Ma ago. Although the obtained ^{39}Ar–^{40}Ar age is significantly higher than the Rb–Sr and Sm–Nd ages, Yamato 000097 shows little or no evidence of trapped Martian atmospheric ^{40}Ar. The trapped ^{40}Ar concentration of Yamato 000097 is similar to that of Zagami, suggesting that both basaltic and lherzolitic shergottites may have similarly inherited excess ^{40}Ar from their magmas.

The Rb–Sr and Sm–Nd ages, and initial $^{87}Sr/^{86}Sr$ and $\varepsilon^{143}Nd$-values of Yamato 000097 and Yamato 793605 lie on the same isotopic ingrowth curves, suggesting that they came from very similar mantle sources. Allan Hills 77005 was also probably derived from the same source, but Lewis Cliff 88516 appears to be from a distinct but similar source. Yamato 000097 represents the most recent known magmatism from its source, and is the youngest Martian meteorite for which concordant Rb–Sr and Sm–Nd ages have been determined.

Keywords: Shergottites; Rb–Sr; Sm–Nd; Crystallization age; Trapped ^{40}Ar

1. Introduction

Yamato (Y) 000027, Y000047, and Y000097 are the eighth lherzolitic shergottite group to be reported. The samples are consist of low-Ca pyroxene, olivine, and maskelynitized plagioclase, with minor amounts of titanomagnetite and phosphates, and show poikilitic and non-poikilitic textures (Imae and Ikeda, 2007; Kojima, 2006; Mikouchi and Kurihara, 2007; Misawa et al., 2006a). Shock effects are prevalent in these meteorites, including shock-melt veins and pockets, maskelynitized plagioclase, and mosaicism of olivine.

Mars ejection ages (i.e., cosmic-ray exposure (CRE) plus terrestrial ages) of lherzolitic shergotites are ~4 Ma (Eugster and Polnau, 1997; Nagao et al.,

* Corresponding author.
E-mail address: misawa@nipr.ac.jp (K. Misawa).

1873-9652/$ - see front matter © 2008 Elsevier B.V. and NIPR. All rights reserved.
doi:10.1016/j.polar.2008.08.001

1997), suggesting that all such meteorites were possibly ejected from Mars by the same impact event (Nyquist et al., 2001). Due to the limited sample size available for isotopic analysis, usually less than 50 g in total weight (except for Allan Hills (ALH) 77005 and Northwest Africa (NWA) 1950), there are few chronological studies of lherzolitic shergottites. Previous Rb–Sr, Sm–Nd, and U–Pb isotopic studies of the lherzolitic shergottites, ALH77005, Y793605, and Lewis Cliff (LEW) 88516 revealed crystallization ages of ~180 Ma, although these meteorites have different initial strontium and neodymium isotopic compositions (Borg et al., 2002; Chen and Wasserburg, 1987, 1993; Jagoutz, 1989; Misawa et al., 1997, 2006b; Morikawa et al., 2001; Shih et al., 1982). Shergottites commonly contain trapped excess ^{40}Ar, which causes their ^{39}Ar–^{40}Ar ages to appear older than ages obtained from the other isotopic systems. Some shocked phases of shergottites contain a trapped Martian atmospheric component, whereas other shergottites may contain ^{40}Ar inherited from the magma (Bogard and Garrison, 1999; Bogard and Park, in press).

As a part of a consortium study of Yamato Martian meteorites, we undertook Rb–Sr, Sm–Nd, and ^{39}Ar–^{40}Ar isotopic analyses of Y000097 to precisely determine its crystallization age and mantle source isotopic signatures. We then compare its isotopic signatures with those of other shergottites, especially the lherzolitic shergottites ALH77005, Y793605, and LEW88516 (Bogard and Garrison, 1999; Borg et al., 2002; Jagoutz, 1989; Misawa et al., 1997, 2006b; Morikawa et al., 2001; Shih et al., 1982). A further aim was to clarify the nature of the shock and alteration events that occurred on the Martian surface and to evaluate crustal evolution on Mars.

2. Sample and analytical procedure

A sample of Y000097,53, weighing ~0.85 g, was processed by initially gently crushing it to <149 μm grain size (Fig. 1). About 25% of the crushed material was used for whole-rock analyses (WR, WR2, and reserve); the remainder was sieved into two size fractions: 149–74 and <74 μm. Mineral separates were obtained from the coarser fraction using a Frantz isodynamic magnetic separator. We obtained a plagioclase-rich sample (Plag) from the non-magnetic fraction, and prepared a pyroxene-rich sample (Px) from the less-magnetic (i.e., moderately magnetic) fraction, from which we removed plagioclase using a heavy liquid with a density $\rho = 2.85\ \mathrm{g\,cm^{-3}}$. We were unable to obtain a pure olivine separate from the magnetic fraction: it also contained pyroxene; we therefore designate this fraction as Ol + Px. For comparison, we also processed three whole-rock samples of Y-793605,71 (Fig. 1).

With the exception of the Px sample, the whole-rock and mineral-concentrate samples were washed with 2 N HCl in an ultrasonic bath for 10 min to leach out possible terrestrial contamination and phosphates. The Px sample was washed with 0.5 N HCl. We analyzed acid residues (WR(r), Px(r), Ol + Px(r), Plag(r)) and leachates (WR(l) and ΣMin(l): combined mineral leachates), unleached whole-rock samples (WR1 from the homogeneous powdered sample Y000097,21 and WR2 from Y000097,53), and whole-rock samples from Y-793605,71 (WR1, WR2, WR(r) and WR(l)) for Rb–Sr and Sm–Nd, following the separation procedures of Shih et al. (1999).

All isotopic measurements were made using Finnigan-MAT multi-collector mass spectrometers (model 261 or 262) following the procedures described by Shih et al. (1999). The average value of ^{87}Sr/^{86}Sr measured for NBS 987 during the course of the study was 0.710266 ± 0.000015 ($2\sigma_p$, σ_p = standard deviation of the population) for a first series of eight analyses, 0.710262 ± 0.000016 for a second series of eight analyses and 0.710248 ± 0.000009 for a third series of one analysis including a single analysis of Y000097. The ^{87}Sr/^{86}Sr results reported here were renormalized to ^{87}Sr/^{86}Sr = 0.710250 for NBS 987 (Nyquist et al., 1994). Samarium and neodymium were analyzed as Sm^+ and NdO^+, respectively. The average value of ^{143}Nd/^{144}Nd during the course of the study for our Ames neodymium standard, which has the same neodymium isotopic composition as the Caltech neodymium standard n(Nd)β (Wasserburg et al., 1981), was 0.511153 ± 0.000017 ($2\sigma_p$) normalized to ^{146}Nd/^{144}Nd = 0.724140 for a first series of twenty-five analyses, 0.511167 ± 0.000021 ($2\sigma_p$) for a second series of ten analyses and 0.511154 ± 0.000027 for a third series of ten analyses. The ^{143}Nd/^{144}Nd values reported here for samples were further normalized to ^{143}Nd/^{144}Nd = 0.511138 for the Caltech neodymium standard n(Nd)β (Wasserburg et al., 1981). The neodymium isotopic measurements for the WR(r) sample of Y000097 and the WR1 sample of Y793605 were unsuccessful due to small sample size or technical problems, and the neodymium isotopic composition for Ol + Px(r) was obtained with large errors.

A 14 mg sample of the plagioclase separate of Y000097,84 was irradiated, along with other meteorite samples and ten NL–25 hornblende age and flux monitors, in a research reactor at the University of

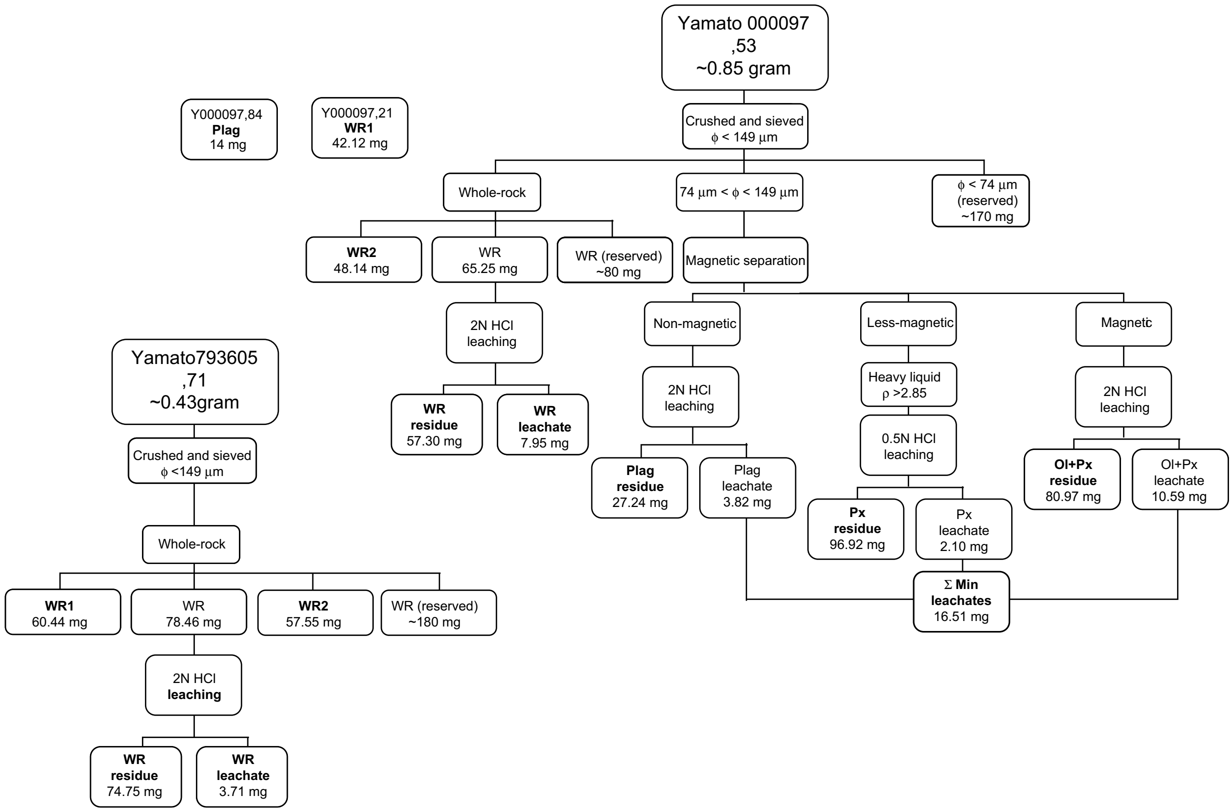

Fig. 1. Flow diagram of sample processing. The whole-rock samples were washed with 2 N HCl in an ultrasonic bath for 10 min. Magnetic separation was performed using a Frantz isodynamic separator. The pyroxene (Px) fraction was purified by density separation using the heavy liquid bromoform (density $\rho = 2.85$ g cm^{-3}). WR = whole-rock, Px = pyroxene, Plag = plagioclase, Ol + Px = olivine separate containing some pyroxene, $\sum$Min leachates = combined mineral leachates.

Missouri, USA. The irradiation constant (*J*-value) measured for this sample was 0.02345 ± 0.00008. Argon was degassed in increasing temperature steps in a tantalum furnace and its isotopic composition was measured using a VG-3600 mass spectrometer at the NASA Johnson Space Center, Texas, USA. Experimental details are given in Bogard et al. (2000).

3. Results

3.1. Rubidium–strontium systematics

Table 1 lists the rubidium and strontium data obtained for Y000097 and Y793605, while Fig. 2 shows rubidium and strontium concentrations for whole-rock and mineral samples for Y000097 and other lherzolitic shergottites. The strontium concentration of WR2(,53) is ∼90% higher than that of WR1(,21), reflecting a greater proportion of the non-poikilitic portion in sub-sample Y000097,53 compared with the homogeneous sample Y000097,21. The rubidium concentrations of the unleached whole-rock samples, WR1(,21) and WR2(,53), are comparable with those of other lherzolitic shergottites (Borg et al., 2002; Dreibus et al., 1992; Gillet et al., 2005; Jagoutz, 1989; Morikawa et al., 2001; Shih et al., 1982). The concentration of strontium in Plag(r) is 346 ppm, approximately three times that in other maskelynitized plagioclase samples from ALH77005 and LEW88516 (Borg et al., 2002; Jagoutz, 1989; Shih et al., 1982), as determined by isotope dilution mass spectrometry. Data for whole-rock leachates (Y79 WR(l) and Y00 WR(l)) and combined acid leachate (ΣMin(l)) plot to the left of the acid residues, along an apparent mixing line (dashed line in Fig. 2). The above observations suggest a component with Rb ≥0.61 ppm and Sr ≥15 ppm and a nearly constant Rb/Sr ratio of ∼0.048, and as well as a second component with Rb ≤0.29 ppm and Sr ≤8.4 ppm, and somewhat lower Rb/Sr ratio, assuming the same components are also present in the Y793605 leachate, Y79 WR(l). The apparent mixing line, if extended to Rb = ∼0, has a non-zero strontium

Table 1
Rb–Sr data for Yamato 000097 and Yamato 793605

Sample[a]	Weight (mg)	Rb (ppm)	Sr (ppm)	$^{87}Rb/^{86}Sr$[b]	$^{87}Sr/^{86}Sr$[b,c]
Yamato 000097					
WR1(,21)	42.12	0.767	10.4	0.2138 ± 24	0.710871 ± 10
WR2(,53)	48.14	0.966	19.4	0.1438 ± 18	0.710727 ± 10
WR(r)	57.30	1.01	18.8	0.1563 ± 21	0.710767 ± 11
WR(l)	7.95	0.432	12.0	0.10387 ± 96	0.710601 ± 10
Plag(r)	27.24	3.87	346	0.03234 ± 34	0.710574 ± 10
Ol + Px(r)	80.97	0.616	6.51	0.2736 ± 47	0.711046 ± 21
Px(r)	96.92	0.344	3.51	0.2838 ± 40	0.711105 ± 10
ΣMin(l)	16.51	0.611	15.2	0.1162 ± 11	0.710644 ± 27
NBS 987 Sr standard, Sr^+ (8 analyses; Mar–Apr, 2007):					0.710262 ± 16[d]
Yamato 793605,71					
WR1	60.44	0.600	8.39	0.2071 ± 29	0.710908 ± 10
NBS 987 Sr standard, Sr^+ (8 analyses; May, 2005):					0.710266 ± 15[d]
WR(r)	74.75	0.630	8.34	0.2184 ± 27	0.710940 ± 16
NBS 987 Sr standard, Sr^+ (8 analyses; Mar–Apr, 2007):					0.710262 ± 16[d]
WR2	57.55	0.672	8.68	0.2241 ± 35	0.710934 ± 10
WR(l)	3.71	0.290	8.41	0.0998 ± 11	0.710696 ± 14
NBS 987 Sr standard, Sr^+ (1 analysis; May, 2007):					0.710248 ± 9[d]

[a] WR = whole-rock, Plag = maskelynitized plagioclase, Ol + Px = olivine separate containing some pyroxene, Px = pyroxene, r = acid residue, l = acid leachate, ΣMin(l) = combined mineral leachates (see Fig. 1).
[b] Uncertainties correspond to last digits and represent $\pm 2\sigma_m$ error limits.
[c] Normalized to $^{88}Sr/^{86}Sr = 8.37521$ and adjusted to $^{87}Sr/^{86}Sr = 0.710250$ of the NBS 987 Sr standard (Nyquist et al., 1994).
[d] Uncertainties correspond to last digits and represent $\pm 2\sigma_p$ error limits.

intercept of ∼2.5. Assuming two-component mixing, one of the components involved must be phosphates. The other component could be an external contaminant of Martian or terrestrial origin. This result was suspected *a priori*, and is one of the reasons why the mineral separates were "cleaned" by leaching. Alternatively, the linear correlation observed between rubidium and strontium could be due to natural abundance variations among phosphates of varying types.

Although the other mineral concentrates show a generally linear trend, this trend could be interpreted as predominantly due to contributions from the major minerals plagioclase (maskelynite), pyroxene, and olivine. The latter two minerals have much lower abundances of both rubidium and strontium than does plagioclase: consequently, the general linear trend can be interpreted to represent data plotting within a mixing triangle that is strongly elongated in the plagioclase direction (i.e., toward high values of rubidium and strontium). Because the sampled phases represent several components, it is unlikely that any linear correlation exhibited by the isotopic data could be a mixing line rather than an isochron.

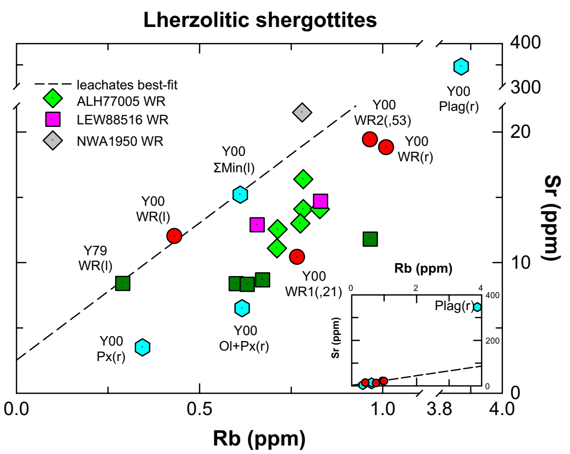

Fig. 2. Rubidium and strontium contents of lherzolitic shergottites analyzed in the present study (Y000097 and Y793605) and previous studies. Data are from Shih et al. (1982), Jagoutz (1989), Morikawa et al. (2001), Borg et al. (2002), Dreibus et al. (1992), Gillet et al. (2005) and this study. Y79 = Y793606, Y00 = Y000097, WR = whole-rock, Px = pyroxene, Plag = plagioclase, Ol + Px = olivine separate containing some pyroxene, ∑Min(l) = combined mineral leachates, r = residue, l = leachate. Three leachate data points (Y79 WR(l), Y00 WR(l), and Y00 ΣMin(l)) plot along an apparent mixing line (dashed line). The inset shows the entire compositional space (note the broken axes in the main figure).

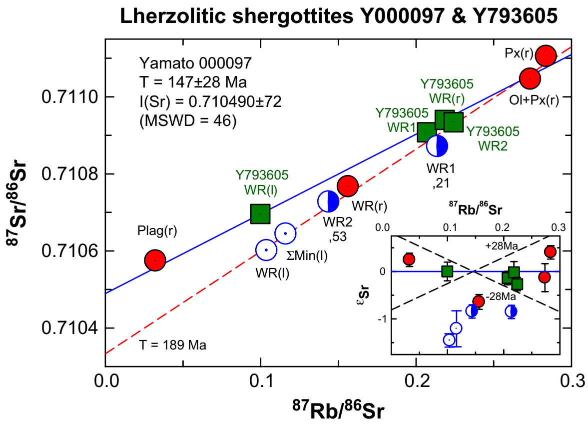

Fig. 3. Rubidium and strontium data for Y000097 (circles) and Y793605 (squares). Y000097 data for residue samples after leaching (filled circles) define a linear array corresponding to a Rb–Sr age of 147 ± 28 Ma with an initial $^{87}Sr/^{86}Sr$ of 0.710490 ± 0.000072. Data points for whole-rock samples of Y793605 also plot on the isochron. The whole-rock and leachate data points do not fit a single isochron, suggesting a minor isotopic disturbance. If the Plag(r) point is excluded and the remaining data are fitted (dashed line), the age becomes 189 ± 18 Ma (MSWD = 9.9), with an initial $^{87}Sr/^{86}Sr = 0.710333 \pm 0.000047$. The inset shows deviations of $^{87}Sr/^{86}Sr$ in parts in 10^4 (ε-units) for whole-rock and mineral samples of Y000097 and Y793605 relative to the 147 Ma isochron. Dashed lines on either side of the best fit line (blue line) correspond to ±28 Ma. WR = whole-rock, Px = pyroxene, Plag = plagioclase, Ol + Px = olivine separate containing some pyroxene, ∑Min(l) = combined mineral leachates, r = residue, l = leachate.

Fig. 3 shows rubidium and strontium data for Y000097, as well as isotopic data for Y793605 for comparison. The eight data points for Y000097 define a linear array corresponding to a Rb–Sr age of 152 ± 31 Ma with an initial $^{87}Sr/^{86}Sr$ of 0.710441 ± 0.000076 (mean square of weighted deviates (MSWD) = 73) for $\lambda(^{87}Rb) = 1.402 \times 10^{-11}\ yr^{-1}$ using the regression program of Williamson (1968); however, the Rb–Sr system of Y000097 is slightly disturbed. This disturbance probably affected the phosphate-enriched leachates most severely, particularly as the data for a similar leachate of Y793605 plot above those data for the Y000097 leachates (see Fig. 3) and are collinear with the major mineral data. A regression line fitted only to residues after leaching, (i.e., Plag(r), WR(r), Ol + Px(r), and Px(r)) gives an age of 147 ± 28 Ma (MSWD = 46) and an initial $^{87}Sr/^{86}Sr = 0.710490 \pm 0.000072$. Alternatively, the Plag(r) point may be excluded and the remaining data fitted, yielding an older age of 189 ± 18 Ma (MSWD = 9.9) with an initial $^{87}Sr/^{86}Sr = 0.710333 \pm 0.000047$. In this latter case, the Plag(r) point deviates upward by +2.2ε-units from the 189 Ma isochron. We do not favor this interpretation because the data from the major mineral phases are considered likely to be more robust than those from phosphate and because a disturbance of the phosphate data could also potentially affect the data for unleached bulk samples. An isochron fitted only to data for the major minerals (i.e., Plag(r), Ol + Px(r), and Px(r)) gives an age of 148 ± 12 Ma (MSWD = 8.1) and an initial $^{87}Sr/^{86}Sr = 0.710507 \pm 0.000033$ with all data falling within the error limits of the isochron. This result, although derived from a subset of the data, is arguably the most robust Rb–Sr age.

3.2. Samarium–neodymium systematics

Table 2 lists the samarium and neodymium data for Y000097 and Y793605. Concentrations of the homogeneous sample WR1(,21) are in good agreement with the results of instrumental neutron activation analysis (INAA) by Shirai and Ebihara (2007) (Fig. 4). The samarium and neodymium contents of WR2(,53) are ~30% higher than those of WR1(,21), suggesting again that Y000097,53 contains a greater proportion of non-poikilitic lithology of the rock and/or a greater abundance of phosphates. Note also that higher samarium and neodymium abundances in WR2(,53) compared with WR1(,21) are accompanied by higher rubidium and strontium abundances (Table 1). In particular, the concentration of strontium in WR2(,53) is nearly twice that in WR1(,21), whereas the rubidium concentration is only ~25% higher, resulting in a lower $^{87}Rb/^{86}Sr$ ratio (Table 1, Fig. 3).

The lherzolitic shergottites analyzed in previous studies have extremely similar fractionated rare earth element (REE) patterns, except that the REE abundances are variable (e.g., NWA1950 are 40–80% higher than those of other lherzolitic shergottites; Gillet et al., 2005). This feature clearly indicates that the REE carrier phases (i.e., Ca-phosphates) in lherzolitic shergottites are distributed very heterogeneously. The CI-chondrite normalized Sm/Nd ratio ($(Sm/Nd)_{CI}$) of Px(r) is 3.14, comparable with the Sm/Nd ratio of PX1(r)[1] of Y793605 ($(Sm/Nd)_{CI} = 3.25$, Misawa et al., 2006b) and within the range of Ca-rich

[1] During the course of the study, the senior author found that the sample names of OL and PX1 described in Misawa et al. (1997, 2006b) and Morikawa et al. (2001) were accidentally mislabeled and exchanged. The U–Th–Pb, Rb–Sr and Sm–Nd ages as well as the main conclusions obtained using these data, however, did not change. Revised tables are available upon request to the senior author.

Table 2
Sm–Nd data for Yamato 000097 and Yamato 793605

Sample[a]	Weight (mg)	Sm (ppm)	Nd (ppm)	$^{147}Sm/^{144}Nd$[b]	$^{143}Nd/^{144}Nd$[b,c]
Yamato 000097					
WR1(,21)	42.12	0.398	0.661	0.36441 ± 41	0.512610 ± 27
WR2(,53)	48.14	0.522	0.881	0.35810 ± 38	0.512610 ± 10
WR(r)	57.30	0.0592	–	–	Failed
WR(l)	7.95	3.82	6.68	0.34528 ± 37	0.512584 ± 10
Plag(r)	27.24	0.0609	0.143	0.2569 ± 11	0.512509 ± 47
Ol + Px(r)	80.97	0.0158	0.0242	0.3947 ± 26	(0.51250 ± 10)
Px(r)	96.92	0.134	0.132	0.61375 ± 97	0.512861 ± 22
ΣMin(l)	16.51	3.62	6.33	0.34558 ± 39	0.512613 ± 17
Ames Nd standard, NdO^+ (10 analyses; May, 2007):					0.511154 ± 27[d]
Yamato 793605,71					
WR1	60.44	0.255	–	–	Failed
Ames Nd standard, NdO^+ (25 analyses; Nov–Dec, 2005):					0.511153 ± 17[d]
WR2	57.55	0.241	0.378	0.38514 ± 56	0.512653 ± 10
Ames Nd standard, NdO^+ (10 analyses; Feb, 2007):					0.511167 ± 21[d]
WR(r)	74.75	0.138	0.151	0.5514 ± 10	0.512764 ± 52
WR(l)	3.71	4.24	7.45	0.34461 ± 39	0.512593 ± 21
Ames Nd standard, NdO^+ (10 analyses; May, 2007):					0.511154 ± 27[d]

[a] WR = whole-rock, Plag = maskelynitized plagioclase, Ol + Px = olivine separate containing some pyroxene, Px = pyroxene, r = acid residue, l = acid leachate, ΣMin(l) = combined mineral leachates (see Fig. 1).
[b] Uncertainties correspond to last digits and represent $\pm 2\sigma_m$ error limits.
[c] Normalized to $^{146}Nd/^{144}Nd = 0.724140$ and adjusted to $^{143}Nd/^{144}Nd = 0.511138$ of the Ames Nd standard (Wasserburg et al., 1981).
[d] Uncertainties correspond to last digits and represent $\pm 2\sigma_p$ error limits.

pyroxene analyzed previously by ion microprobe (Harvey et al., 1993; Lundberg et al., 1990). Enrichments of samarium and neodymium in acid leachates of Y000097 (WR(l) and ΣMin(l)) are 25× and 14×

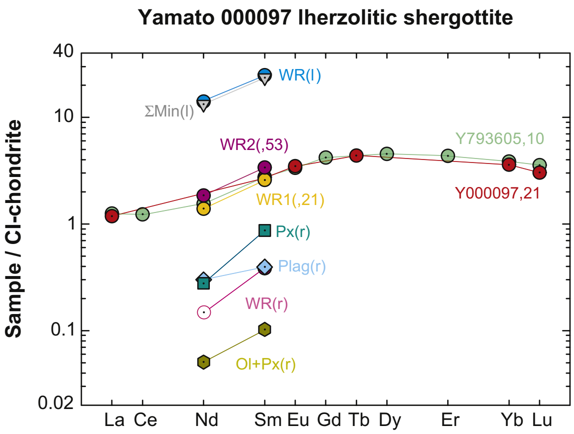

Fig. 4. CI-chondrite normalized samarium and neodymium abundances of whole-rock and mineral samples for Y000097. Also shown are the REE patterns for Y000097,21 (INAA data; Shirai and Ebihara, 2007) and Y793605,10 (Misawa et al., 2006b). The neodymium abundance of WR(r) (open circle) was calculated from a mass balance of WR(l) and WR2(,53).

CI-chondrite, respectively. About 90% of the samarium and neodymium were leached from the whole-rock sample of Y000097; however, just 60–70% of the samarium and neodymium were leached from the whole-rock sample of Y793605.

The Sm–Nd data obtained for Y000097 and Y793605 are shown in Fig. 5. The six data points for Y000097 define a linear array corresponding to a Sm–Nd age of 152 ± 13 Ma with an initial ε^{143}Nd-value of +11.7 ± 0.2 (MSWD = 2.3) for $\lambda(^{147}Sm) = 6.54 \times 10^{-12}\ yr^{-1}$ using the regression program of Williamson (1968). The Sm–Nd data for the whole-rock samples of Y793605 (WR2, WR(r), and WR(l)) also plot on the Y000097 isochron (see Fig. 5, inset), indicating that the Sm–Nd age for Y793605 is, within error limits, indistinguishable from that of Y000097. The Sm–Nd age obtained for Y000097 is slightly younger than that for Y793605 (185 ± 16 Ma) obtained for acid leachate and residue samples (Misawa et al., 2006b), but is identical to the Rb–Sr age of 152 ± 31 Ma obtained when all the Rb–Sr data are included in the regression, and within error limits of 148 ± 12 Ma obtained when only the most robust data for the major minerals are considered. These results demonstrate that the Sm–Nd isotopic system remained

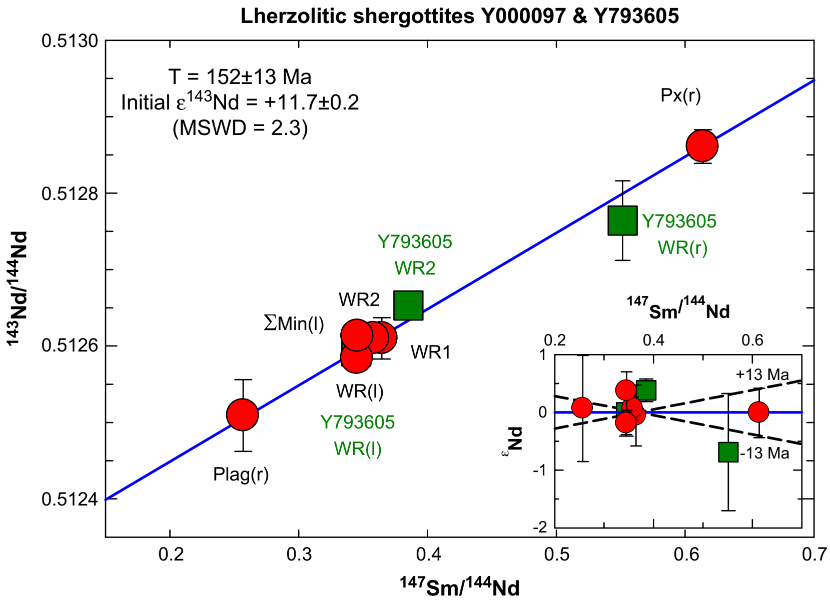

Fig. 5. Samarium and neodymium data for Y000097 (circles) and Y793605 (squares). A total of six data points for Y000097 define a linear array corresponding to a Sm–Nd age of 152 ± 13 Ma with an initial ε^{143}Nd-value of +11.7 ± 0.2. Data points for whole-rock samples of Y793605 also plot on the isochron. The inset shows deviations of ^{143}Nd/^{144}Nd in parts in 10^4 (ε-units) for whole-rock and mineral samples of Y000097 and Y793605 relative to the 152 Ma isochron. Dashed lines on either side of the best fit line (blue line) correspond to ±13 Ma. WR = whole-rock, Px = pyroxene, Plag = plagioclase, ∑Min(l) = combined mineral leachates, r = residue, l = leachate.

robust against the disturbance that affected the Rb–Sr isotopic system of the phosphate minerals.

3.3. ^{39}Ar–^{40}Ar age

In the present study, argon data are provided in Appendix. The ^{39}Ar–^{40}Ar age spectrum for Y000097 plagioclase is shown in Fig. 6. The ^{39}Ar–^{40}Ar age is relatively constant at ~300 Ma throughout the release, and the K/Ca ratio is also nearly constant at 0.03–0.04. We examined these data in an isochron plot (not shown) of ^{40}Ar/^{36}Ar versus ^{39}Ar/^{36}Ar, using cosmogenic ^{36}Ar. From the ^{36}Ar/^{37}Ar ratios, we estimate that those extractions that released the first 5% of ^{39}Ar also released trapped ^{36}Ar; however, ^{36}Ar/^{37}Ar ratios in the remaining extractions were relatively constant, indicating that the released ^{36}Ar was essentially a pure cosmogenic component (Garrison et al., 2000). The total cosmogenic ^{36}Ar in our plagioclase sample was 2.4×10^{-9} cm^3 g^{-1}, similar to the amount of cosmogenic ^{36}Ar measured in several other shergottites. For example, Nagao et al. (2007) reported ^{36}Ar$_{cos}$ in Y000097 whole-rock sample to be $\sim 1.5 \times 10^{-9}$ cm^3 g^{-1} and a CRE age to be 3–5 Myr, similar values and ages reported for other shergottites. Unfortunately, our argon isochron data tend to show a scatter ($R^2 = 0.68$) and relatively small variations in isotopic ratios. Such clustering of the isochron data indicates that all of the ^{40}Ar is distributed throughout the lattice in close association with ^{39}Ar and cosmogenic ^{36}Ar produced from calcium by cosmic-rays. The ^{39}Ar–^{40}Ar age defined by the isochron is ~260 Ma, although the reliability of this age is uncertain.

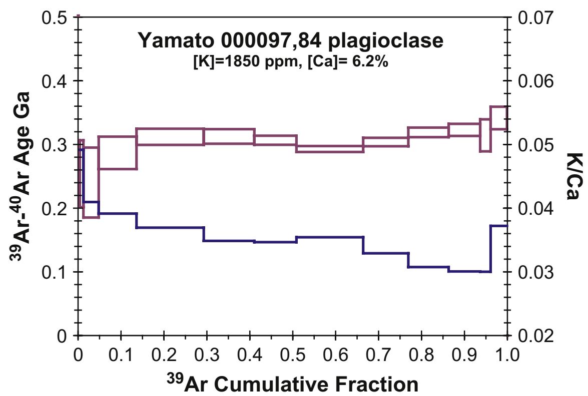

Fig. 6. ^{39}Ar–^{40}Ar ages (rectangles, left-hand scale) and K/Ca ratios (stepped line, right-hand scale) for stepwise temperature extractions of Y000097 plagioclase, plotted as a function of cumulative release of ^{39}Ar.

4. Discussion

4.1. Disturbance of the Rb–Sr isotopic system

The shergottites, including the Y00 lherzolitic samples, suffered intense shock metamorphisms, resulting in deformation, the transformation of plagioclase to maskelynite, generation of high-pressure phases (e.g., Beck et al., 2004; Chen and El Goresy, 2000; Fritz et al., 2005; Stöffler, 2000), and partial meltings. Any of these events could have caused disturbances of their isotopic systems. Aqueous alteration on the Martian surface (Bridges et al., 2001) also may have disturbed the isotopic systems. Furthermore, we must take into account the effects on parent–daughter elemental fractionations during acid leaching.

About 12% of the Y000097 whole-rock sample was dissolved during the 2 N HCl treatment, whereas only 5% of the whole-rock sample of Y793605 was leached out. This difference may be due partly to different shock effects produced during impact(s) on the shergottites because shock brecciation increases the density of microfractures and the surface area of minerals, and may be related to the petrographically heterogeneous characteristics of lherzolitic shergottites.

The near concordance of rubidium and strontium concentrations in 2 N HCl-leached and unleached whole-rock samples (Fig. 2) suggests only minor terrestrial weathering effects on rubidium and strontium, presumably during residency in Antarctic ice, for Y000097 and Y793605. Nevertheless, either terrestrial or Martian weathering, as well as the shock-related effects discussed above, is most likely to have affected the phosphate minerals in these lherzolitic shergottites, consistent with the obtained isotopic data.

The Rb–Sr data for the whole-rock samples of Y793605 (WR1, WR2, WR(r), and WR(l)) plot on the Y000097 isochron (see Fig. 3, inset), suggesting that these lherzolitic shergottites have almost identical crystallization ages. This fact suggests that Y793605 and Y000097 are possibly genetically related, having originated from very similar geological settings on Mars. The Y79 WR(l) data point deviates upward by +1.4ε-units from the 189 Ma isochron that would result for Y000097 if the Rb–Sr isochron were passed through the leachate data rather than Plag(r).

4.2. Enrichment of strontium in maskelynitized plagioclase

A remarkable feature of the analyzed sample is the extremely high strontium abundance of 346 ppm in the acid-washed plagioclase sample, Plag(r). The strontium content of maskelynitized plagioclase in Grove Mountain (GRV) 99027 determined by ion microprobe is only 136 ppm (Lin et al., 2005), comparable with concentrations reported for acid-leached plagioclase fractions from ALH77005 and LEW88516 (Borg et al., 2002). Adhering phosphates/impact melt with maskelynitized plagioclase is in principle a possible explanation of the strontium enrichment observed in Plag(r). The strontium concentration of GRV99027

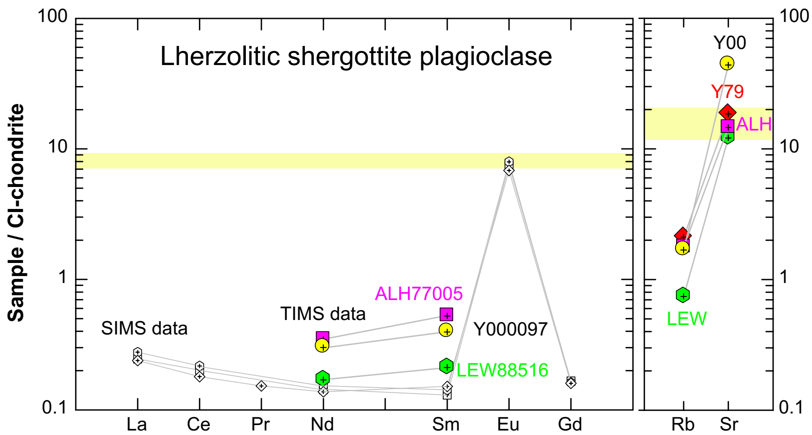

Fig. 7. CI-chondrite normalized light- to middle-REEs, rubidium, and strontium abundances of plagioclase from the lherzolitic shergottites, ALH77005, Y793605, LEW88516, and Y000097. Open and solid symbols represent data obtained by secondary ion probe mass spectrometry (SIMS) and thermal ionization mass spectrometry (TIMS), respectively (Borg et al., 2002; Harvey et al., 1993; Lundberg et al., 1990; Misawa et al., 2006b; Wadhwa et al., 1999). The samarium and neodymium abundances obtained for Y000097 Plag(r) are similar to those in plagioclase determined by SIMS for other lherzolitic shergottites. In general, europium and strontium abundances of lherzolitic shergottites are 7–8× and 12–20× CI-chondrite, respectively (yellow bands). These observations strongly suggest that the enrichment of strontium in Y000097 Plag(r) does not reflect the contribution of phosphates or glass inclusions.

merrillite measured by ion microprobe is ~150 ppm, comparable with the concentration of maskelynitized plagioclase in other shergottites; however, the samarium and neodymium concentrations of Plag(r) are comparable with those of plagioclase from ALH77005 and LEW88516 (Fig. 7). This observation suggests that the Plag(r) fraction does not contain REE-rich phases such as impact-melt glass or phosphates. One hypothetical interpretation of the observed strontium enrichment is that a more evolved component in metasomatic fluids or in secondary alteration products with very high strontium abundance may have been added to and/or adsorbed by plagioclase prior to an intense shock event. Owing to intense shock loading, the altered plagioclase may then have become compacted and transformed into maskelynite. In such a case, Plag(r) would lie on a secondary isochron; however, we interpret the Plag(r) data as lying on a primary isochron, indicating that the strontium enrichment apparent in the maskelynite sample probably occurred during igneous crystallization of the rock.

4.3. Carrier phases of REEs in lherzolitic shergottites

Previous *in situ* ion microprobe analysis of REEs in constituent phases of lherzolitic shergottites, as well as acid leaching experiments of whole-rock samples, revealed that the Ca-phosphates, apatite and merrillite, govern the whole-rock REE pattern (Harvey et al., 1993; Hsu et al., 2004; Lin et al., 2005; Lundberg et al., 1990). Y000097 contains both apatite and merrillite in the non-poikilitic lithology, whereas previous studies were unable to locate coarse-grained phosphates in thin sections of Y793605 (Ikeda, 1997; Mikouchi and Miyamoto, 1997; Wadhwa et al., 1999). Nagao et al. (1997) reported a single merrillite grain adjacent to maskelynitized plagioclase in Y793605, and Mittlefehldt et al. (1997) identified Fe-phosphate and partly decomposed Ca-phosphate grains interpreted to have suffered alteration while in Antarctica.

The Sm/Nd ratios of acid leachates for Y000097 (WR(l) and ΣMin(l)) and Y793605 (WR(l)) are constant ($^{147}Sm/^{144}Nd = 0.345$) and indistinguishable from those of ALH77005 leachates ($^{147}Sm/^{144}Nd = 0.344$; Borg et al., 2002); in contrast, the $^{147}Sm/^{144}Nd$ ratios of acid leachates for LEW88516 are much smaller ($^{147}Sm/^{144}Nd = \sim 0.273$; Borg et al., 2002). The present analytical results suggest no differences among Y000097, Y793605, and ALH77005 in terms of samarium and neodymium abundances in acid

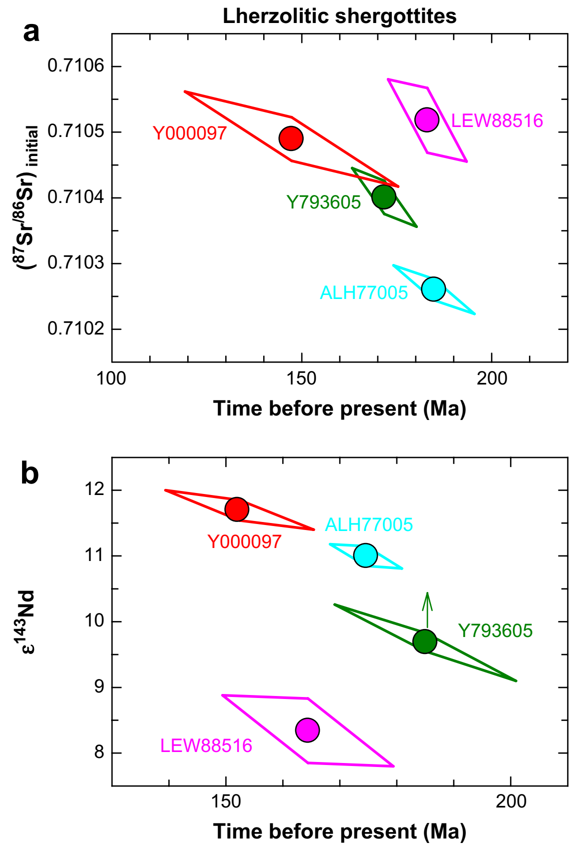

Fig. 8. (a) Age versus initial $^{87}Sr/^{86}Sr$ for lherzolitic shergottites. Data are from Morikawa et al. (2001), Borg et al. (2002), and this study. Ages and initial isotopic ratios were recalculated using the regression program of Williamson (1968). Strontium isotopic ratios are adjusted to $^{87}Sr/^{86}Sr = 0.710250$ for the NBS 987 strontium standard (Nyquist et al., 1994). The error parallelogram for Y000097 overlaps with that for Y793605. (b) Age versus initial ε^{143}Nd-value for lherzolitic shergottites. Data are from Borg et al. (2002), Misawa et al. (2006b), and this study. Ages and initial ε^{143}Nd-values were recalculated using the regression program of Williamson (1968). Neodymium isotopic ratios are adjusted to $^{143}Nd/^{144}Nd = 0.511138$ for the Ames neodymium standard (Wasserburg et al., 1981).

leachates, and that Ca-phosphates, the carrier phases of REEs, are heterogeneously distributed in lherzolitic shergottites, especially in Y793605.

The samarium and neodymium abundances in mineral separates are 2–5 times higher than those determined by ion microprobe in pyroxene and plagioclase, possibly reflecting the fact that components enriched in REEs, especially in heavy REEs, remain in acid residue samples. The CI-normalized Sm/Nd ratios of plagioclase determined by secondary ion mass spectrometry (SIMS) ($(Sm/Nd)_{CI,SIMS} = 0.91-1.1$) are lower than those obtained by thermal ionization mass spectrometry (TIMS) ($(Sm/Nd)_{CI,TIMS} = 1.24-1.52$).

4.4. Crystallization age of Y000097 and isotopic signature of source material

On a plot of Rb–Sr age versus initial $^{87}Sr/^{86}Sr$ (Fig. 8a), the error parallelogram for Y000097 lies on the extension of the radiogenic $^{87}Sr^*$ ingrowth curve for Y793605, but not on those for ALH77005 or LEW88516, suggesting that Y000097 and Y793605 were either co-magmatic or are derived from very similar source regions. In contrast, LEW88516 and possibly ALH77005 appear to have been derived from distinct but similar source regions.

Similarly, on an age versus initial $\varepsilon^{143}Nd$ diagram (Fig. 8b), the error parallelogram for Y000097 is clearly distinct from that for LEW88516, but defines an array with the error parallelograms for ALH 77005 and Y793605. In considering this array, it is necessary to take into account inter-laboratory biases in neodymium isotope measurements, which would raise the initial $\varepsilon^{143}Nd$-value of Y793605 reported by Misawa et al. (2006b) by $\sim+0.5\varepsilon$-units to enable comparison with the data for ALH77005 and Y000097.

4.5. Origin of excess ^{40}Ar in shergottites

Y000097 is the first Martian lherzolitic shergottite for which $^{39}Ar-^{40}Ar$ data yield an apparent age similar to those determined by other chronometers. Most of the $^{39}Ar-^{40}Ar$ ages determined previously for shergottites have been obtained for basaltic meteorites: few such ages have been obtained for lherzolitic shergottites. In a $^{39}Ar-^{40}Ar$ study of whole rock samples of the ALH77005 and Y793605 lherzolitic shergottites, Bogard and Garrison (1999) found that ^{40}Ar shock-implanted from the Martian atmosphere was dominant. Likewise, Walton et al. (2007) found that Martian atmospheric ^{40}Ar is dominant in the lherzolitic shergottites ALH77005 and NWA1950. The authors reported a multiple laser-shot isochron "age" of 382 ± 36 Ma for NWA1950, and a range in ages of 373–8108 Ma for individual laser-shot analyses of ALH77005, representing clear evidence of excess ^{40}Ar; however, we observed little to no evidence of Martian atmospheric ^{40}Ar in the data reported here for Y000097. Nagao et al. (2007) also found little evidence for Martian atmospheric xenon and krypton in their whole-rock samples of Y000097. Our plagioclase sample contained 9.8×10^{-7} cm^3 g^{-1} of excess ^{40}Ar, which 50% of the total ^{40}Ar. This amount of excess ^{40}Ar is similar to the excess ^{40}Ar concentrations of $10-20 \times 10^{-7}$ cm^3 g^{-1} we reported from mineral separates of the Zagami shergottite (Bogard and Park, in press). We suggest that excess ^{40}Ar in Zagami is a radiogenic component inherited either from the original magma or from an early assimilation of crustal material into the magma. Excess ^{40}Ar in Y000097 may have a similar origin. Based on this observed similarity in trapped ^{40}Ar concentrations, we suggest that basaltic and lherzolitic shergottites may have experienced similar magmatic histories, although they differ in the detailed isotopic signatures of certain elements.

5. Conclusion

Isotopic analysis of the Martian lherzolitic shergottite Y000097 yields a Rb–Sr age of 147 ± 28 Ma with an initial $^{87}Sr/^{86}Sr$ ratio of 0.710490 ± 0.000072, a Sm–Nd age of 152 ± 13 Ma with an initial $\varepsilon^{143}Nd$-value of $+11.7 \pm 0.2$, and a $^{39}Ar-^{40}Ar$ age of ~ 260 Ma. The near concordance of these ages and the Rb–Sr and Sm–Nd initial isotopic signatures suggest that Y000097 was produced by partial melting of low Rb/Sr, light-REE depleted source materials ~ 150 Ma ago. The Sm–Nd ages and $\varepsilon^{143}Nd$-values of Y000097, Y793605, and possibly ALH77005 closely overlap, suggesting that they lie on the same radiogenic $^{143}Nd^*$ ingrowth curve or along the very similar curve. This in turn implies that they could have come from very similar mantle sources. In contrast, LEW88516 appears to be derived from a distinct (although similar) source. Y000097 may contain excess ^{40}Ar from the source magma, but shows little or no evidence of Martian atmospheric ^{40}Ar. In contrast, the lherzolitic shergottites ALH77005 and Y793605 contain significant amounts of Martian atmospheric ^{40}Ar.

Acknowledgments

We thank two anonymous reviewers for their helpful suggestions. This work was supported by the NASA Cosmochemistry Program (D.B. and L.E.N.), the NASA Postdoctoral Program (J.P.), NIPR Research Project Funds, P8 (Evolution of the Early Solar System Materials), and a Grant-in-Aid for Scientific Research (No. 17540464 awarded to K.M.).

Appendix 1

Argon isotopic data

Temp. (°C)	^{39}Ar ($\times 10^{-9}$ cm^3 STP g^{-1})	Age (Ma)	K/Ca ratio	$^{40}Ar/^{39}Ar$ (±error)	$^{38}Ar/^{39}Ar$ (±error)	$^{37}Ar/^{39}Ar$ (±error)	$^{36}Ar/^{39}Ar$ (±error)
300	0.016	1020	0.024	32	11	23	1.3
		510	0.017	21	9	17	1.1
400	0.253	420	0.068	11.2	2.2	8.1	0.24
		170	0.035	5.2	1.4	4.2	0.15
500	0.797	550	0.073	15.2	1.11	7.5	0.108
		130	0.022	4.0	0.39	2.2	0.042
600	2.088	254	0.049	6.5	0.94	11.2	0.0239
		53	0.013	1.4	0.29	2.9	0.0094
700	9.002	240	0.041	6.1	0.61	13.4	0.0234
		55	0.012	1.5	0.21	3.8	0.0091
800	22.31	287	0.039	7.35	0.262	14.1	0.0111
		25	0.004	0.70	0.036	1.6	0.0021
880	39.62	312	0.037	8.05	0.182	14.89	0.0117
		13	0.002	0.36	0.012	0.78	0.0012
920	29.77	313	0.035	8.07	0.155	15.78	0.0139
		12	0.002	0.32	0.009	0.74	0.0013
960	24.82	307	0.035	7.90	0.158	15.87	0.0141
		7.2	0.001	0.20	0.006	0.50	0.0012
1010	39.32	293	0.035	7.52	0.171	15.52	0.0119
		4.7	0.001	0.13	0.005	0.35	0.0008
1060	26.61	304	0.033	7.82	0.330	16.71	0.0099
		6.7	0.001	0.19	0.011	0.49	0.0009
1110	23.75	319	0.031	8.25	0.330	17.89	0.0110
		7.6	0.001	0.21	0.012	0.56	0.0010
1180	18.60	323	0.030	8.36	0.270	18.29	0.0151
		9.5	0.001	0.27	0.013	0.70	0.0014
1280	6.169	314	0.030	8.12	0.273	18.3	0.0154
		25	0.003	0.71	0.034	1.8	0.0032
1400	9.609	342	0.037	8.89	0.232	14.78	0.0110
		18	0.002	0.50	0.019	0.97	0.0019
1500	0.266	95	0.051	2.3	0.016	10.7	0.0200
		47	0.029	1.2	0.011	6.1	0.0120

A 14 mg sample of the plagioclase separate of Yamato 000097,84 was analyzed. Columns (left to right) indicate extraction temperature in °C, ^{39}Ar concentrations (units 10^{-9} cm^3 STP g^{-1}), age in Ma, K/Ca ratio, and isotopic ratios relative to ^{39}Ar. Uncertainties in age, K/Ca, and isotopic ratios are given beneath each value.

References

Beck, P., Gillet, P., Gautron, L., Daniel, I., El Goresy, A., 2004. A new natural high-pressure (Na,Ca)-hexaluminosilicate [$(Ca_xNa_{1-x})Al_{3+x}Si_{3-x}O_{11}$] in shocked Martian meteorites. Earth Planet. Sci. Lett. 219, 1−12.

Bogard, D.D., Garrison, D.H., 1999. Argon-39−argon-40 “ages” and trapped argon in Martian shergottites, Chassigny, and Allan Hills 84001. Meteoritics Planet. Sci. 34, 451−473.

Bogard, D.D., Park, J. ^{39}Ar−^{40}Ar dating of the Zagami Martian shergottite and implications for magma origin of excess ^{40}Ar. Meteoritics Planet. Sci., in press.

Bogard, D.D., Garrison, D.H., McCoy, T.J., 2000. Chronology and petrology of silicates from IIE iron meteorites: evidence of a complex parent body evolution. Geochim. Cosmochim. Acta 64, 2133−2154.

Borg, L.E., Nyquist, L.E., Wiesmann, H., Reese, Y., 2002. Constraints on the petrogenesis of Martian meteorites from the Rb−Sr and Sm−Nd isotopic systematics of the lherzolitic shergottites ALH 77005 and LEW 88516. Geochim. Cosmochim. Acta 66, 2037−2053.

Bridges, J.C., Catling, D.C., Saxton, J.M., Swindle, T.D., Lyon, I.C., Grady, M.M., 2001. Alteration assemblages in Martian meteorites: implication for near-surface processes. Space Sci. Rev. 96, 365−392.

Chen, J.H., Wasserburg, G.J., 1987. S ≠ N= ?C. Lunar Planet. Sci. XVII, 113−114 (abstract).

Chen, J.H., Wasserburg, G.J., 1993. LEW 88516 and SNC meteorites. Lunar Planet. Sci. XXIV, 275−276 (abstract).

Chen, M., El Goresy, A., 2000. The nature of maskelynite in shocked meteorites: not diaplectic glass but a glass quenched from shock-induced dense melt at high pressures. Earth Planet. Sci. Lett. 179, 489−502.

Dreibus, G., Jochum, K.H., Palme, H., Spettel, B., Wlotzka, F., Wänke, H., 1992. LEW 88516: a meteorite compositionally close to the “Martian mantle. Meteoritics 27, 216−217 (abstract).

Eugster, O., Polnau, E., 1997. Mars−Earth transfer time of lherzolite Yamato-793605. Antarct. Meteorite Res. 10, 143−149.

Fritz, J., Artemieva, N., Greshake, A., 2005. Ejection of Martian meteorites. Meteoritics Planet. Sci. 40, 1393−1411.

Garrison, D.H., Hamlin, S., Bogard, D.D., 2000. Chlorine abundances in meteorites. Meteoritics Planet. Sci. 35, 419−425.

Gillet, P., Barrat, J.A., Beck, P., Marty, B., Greenwood, R.C., Franchi, I.A., Bohn, M., Cotten, J., 2005. Petrology, geochemistry, and cosmic-ray exposure age of lherzolitic shergottite Northwest Africa 1950. Meteoritics Planet. Sci. 40, 1175−1184.

Harvey, R.P., Wadhwa, M., McSween Jr., H.Y., Crozaz, G., 1993. Petrography, mineral chemistry and petrogenesis of Antarctic shergottite LEW 88516. Geochim. Cosmochim. Acta 57, 4769−4783.

Hsu, W., Guan, Y., Wanf, H., Leshin, L.A., Wang, R., Zhang, W., Chen, X., Zhang, F., Lin, C., 2004. The lherzolitic shergottite Grove Mountains 99027: rare earth element geochemistry. Meteortitics Planet. Sci. 39, 701−709.

Ikeda, Y., 1997. Petrology and mineralogy of the Y-793605 Martian meteorite. Antarct. Meteorite Res. 10, 13−40.

Imae, N., Ikeda, Y., 2007. Petrography of new lherzolitic shergottites of Yamato 000027, Y000047, and Y000097: main lithologies and shock veins. Antarct. Meteorites XXXI, 32−33 (abstract).

Jagoutz, E., 1989. Sr and Nd isotopic systematics in ALHA 77005: age of shock metamorphism in shergottites and magmatic differentiation on Mars. Geochim. Cosmochim. Acta 46, 2429−2441.

Kojima, H. (Ed.), 2006. Meteorite Newsletter 14, 1−5.

Lin, Y., Guan, Y., Wang, D., Kimura, M., Leshin, L.A., 2005. Petrogenesis of the new lherzolitic shergottite Grove Mountains 99027: constraints of petrography, mineral chemistry, and rare earth elements. Meteoritics Planet. Sci. 40, 1599−1619.

Lundberg, L.L., Crozaz, G., McSween, H.Y., 1990. Rare earth elements in minerals of the ALH 77005 shergottite and implications for its parent magma and crystallization history. Geochim. Cosmochim. Acta 54, 2535−2547.

Mikouchi, T., Miyamoto, M., 1997. Yamato-793605: A new lherzolitic shergottite from the Japanese Antarctic meteorite collection. Antarct. Meteorite Res. 10, 13−40.

Mikouchi, T., Kurihara, T., 2007. Y000027, Y000047, and Y000097: mineralogy and petrology of paired Yamato 00 lherzolitic shergottites. Antarct. Meteorites XXXI, 52−53 (abstract).

Misawa, K., Iwata, N., Imae, N., Franchi, I.A., Greenwood, R.C., Kojima, H., 2006a. New lherzolitic shergottites from the Yamato Mountains. Antarct. Meteorites XXX, 63–64 (abstract).

Misawa, K., Nakamura, N., Premo, W.R., Tatsumoto, M., 1997. U–Th–Pb isotopic systematics of lherzolitic shergottite Yamato-793605. Antarct. Meteorite Res. 10, 95–108.

Misawa, K., Yamada, K., Nakamura, N., Morikawa, N., Yamashita, K., Premo, W.R., 2006b. Sm–Nd isotopic systematics of lherzolitic shergottite Yamato-793605. Antarct. Meteorite Res. 19, 45–57.

Mittlefehldt, D.W., Wentworth, S.J., Wang, M.-S., Lindstrom, M.M., Lipschutz, M.E., 1997. Geochemistry of and alteration phases in Martian lherzolite Y-793605. Antarct. Meteorite Res. 10, 109–124.

Morikawa, N., Misawa, K., Kondorosi, G., Premo, W.R., Tatsumoto, M., Nakamura, N., 2001. Rb–Sr isotopic systematics of lherzolitic shergottite Yamoto-793605. Antarct. Meteorite Res. 14, 47–60.

Nagao, K., Nakamura, T., Miura, Y.N., Takaoka, N., 1997. Noble gases and mineralogy of primary igneous materials of the Yamayo-793605 shergottite. Antarct. Meteorite Res. 10, 125–142.

Nagao, K., Park, J., Choi, H., 2007. Noble gases of the Yamato 000027 and Yamato 000097 lherzolitic shergottites. Antarct. Meteorites XXXI, 62–63 (abstract).

Nyquist, L.E., Bansal, B., Wiesmann, H., Shih, C.-Y., 1994. Neodymium, strontium, and chromium isotopic studies of the LEW 86010 and Angra dos Reis meteorites and the chronology of the angraite parent body. Meteoritics Planet. Sci. 29, 872–885.

Nyquist, L.E., Bogard, D.D., Shih, C.-Y., Greshake, A., Stöffler, D., Eugster, O., 2001. Ages and geologic histories of Martian meteorites. Space Sci. Rev. 96, 105–164.

Shih, C.-Y., Nyquist, L.E., Bogard, D.D., McKay, G.A., Wooden, J.L., Bansal, B.M., Wiesmann, H., 1982. Chronology and petrogenesis of young achondrites, Shergotty, Zagami, and ALHA 77005: late magmatism on a geologically active planet. Geochim. Cosmochim. Acta 46, 2323–2344.

Shih, C.-Y., Nyquist, L.E., Wiesmann, H., 1999. Samarium–neodymium and rubidium–strontium systematics of nakhlite Governador Valadares. Meteoritics Planet. Sci. 34, 647–655.

Shirai, N., Ebihara, M., 2007. Chemical characteristics of lherzolitic shergottite Yamato 000097. Antarct. Meteorites XXXI, 91–92.

Stöffler, D., 2000. Maskelynite confirmed as diaplectic glass: indication for peak shock pressures below 45 GPa in all Martian meteorites. 31st Lunar Planetary Science Conference, #1170 (abstract).

Wadhwa, M., McKay, G.A., Crozaz, G., 1999. Trace element distributions in Yamato-793605, a chip of the "Martian lherzolite" block. Antarct. Meteorite Res. 12, 168–182.

Walton, E.L., Kelly, S.P., Herd, C.D.K., 2007. A laser probe $^{40}Ar-^{39}Ar$ investigation of two Martian lherzolitic shergottites. Meteoritics Planet. Sci. 42, A159 (abstract).

Wasserburg, G.J., Jacobsen, S.B., DePaolo, D.J., McCulloch, M.T., Wen, T., 1981. Precise determination of Sm/Nd ratios, Sm and Nd isotopic abundances in standard solutions. Geochim. Cosmochim. Acta 45, 2311–2323.

Williamson, J.H., 1968. Least-squares fitting of a straight line. Can. J. Phys. 46, 1845–1847.